On the Uplink SIR Distributions in Heterogeneous Cellular Networks

Hyung Yeol Lee, *Student Member, IEEE*, Young Jin Sang, *Member, IEEE*, and Kwang Soon Kim, *Senior Member, IEEE*

***Abstract*—In this paper, the uplink (UL) signal-to-interference ratio (SIR) distributions in a two-tier heterogeneous cellular network (HCN) are analyzed by considering the power control effect and approximating the UL interferer locations as a non-uniform Poisson point process (PPP). Approximated closed-form SIR distributions are provided according to the tier, association rule, power control strategy for each tier, and resource partition (common or dedicated) and are shown to be quite close to the true distributions in a wide range of network parameters.**

***Index Terms*—Cell association, HCN, uplink (UL) signal-to-interference ratio (SIR) distribution.**

I. Introduction

RECENTLY, small-cell base stations (BSs) are deployed on existing wireless cellular networks, called an HCN [1], to provide higher end-user throughput with low cost. In such an HCN, although the wireless channel quality in each tier, represented by the SIR distribution, does not change in downlink (DL) [2], load imbalance can be caused from different cell coverage as derived in [3] and an appropriate load balancing scheme, such as in [4], is essential so that a cell range expansion with enhanced inter-cell interference coordination has been adopted in the 3GPP long term evolution advanced. When such a load balancing is applied in an HCN, analytical framework, such as in [4] for DL HCN, provides not only profound understanding on the DL characteristics in an HCN but also a theoretical background for optimizing real cellular networks. However, although UL is as important as DL, it has been less focused.

In UL, the interference characteristic is quite different from that in DL due to the fact that an interferer can be closer to the desired transmitter and that a transmit power control is used. In an HCN, such differences become more severe so that tier-m users (users associated to a macro-cell) may suffer from stronger interference caused by tier-s users (users associated to a small-cell) within its BS coverage, which may require different power control strategies in different tiers. Thus, an accurate analytical framework, comparable to that in DL, is required. In [5], the UL SIR distribution of a single-tier network was derived by assuming the UL interferer distribution follows a homogeneous PPP. However, the UL interferer location is highly non-uniform and even dependent on the BS realizations, which are not fully considered in [5]. In [6], approximated UL SIR distributions of a two-tier code division multiple access (CDMA) system are investigated. However, it is hard to use the result directly for a system using orthogonal multiple access such as orthogonal frequency division multiple access (OFDMA) by simply setting unit processing gain because the interference from each interfering cell in such a system is sensitive on the interferer location while that in a CDMA system is averaged over multiple interferers in each cell. Therefore, more accurate analysis is required to fully understand the UL characteristics in an HCN, which can be utilized to devise better association, load balancing, power control and resource allocation schemes for UL.

In this paper, to analyze the UL SIR distribution, the distribution on the UL interferer locations is approximated as a non-uniform PPP and closed-form SIR distributions according to the association, power control and resource partitioning schemes are derived. By utilizing the proposed analytic framework, the impact of the cell association, power control strategy, and resource partitioning schemes on the network behavior can be easily anticipated in terms of the SIR distributions, which can provide better understanding on the UL HCN and a theoretical background for advanced schemes for the UL HCN.

TABLE I
Summary on the Notations

Symbol	Description
Indices k, r, z	Tier $k \in \{m, s\}$, resource $r \in \{c, d\}$, link-$z \in \{D, U\}$
$\mathbf{Y}_k$, $\mathbf{y}^z(\mathbf{x})$	Tier-k BS set, the associated BS of user $\mathbf{x}$ in link-z
$\mathbf{X}^z(\mathbf{y})$, $\mathbf{x}^z(\mathbf{y})$, $\mathbf{X}_k^z$	Set of users associated to BS $\mathbf{y}$ in link-z, the randomly selected user by $\mathbf{y}$ in link-z, tier-k user set in link-z
$P_k, P_u(\mathbf{x})$	Transmit power of tier-k BS, transmit power of user $\mathbf{x}$
A_k, A_u, κ_k^z	Tier-k antenna gain, user antenna gain, tier-k biasing factor in link-z
ζ_k^z, ζ_c^z	Tier-k dedicated resource portion in link-z, common resource portion in link-z
γ_k (η_k)	Tier-k UL target SNR (power)
$\Gamma_{\mathbf{y},r}^z$	Selected user's SIR in BS $\mathbf{y}$ using resource r in link-z
$\mathcal{S}_{k,r}^z(T)$	Tier-k SIR distribution using resource r in link-z
$\bar{\lambda}_k(\lambda_k)$, λ_u	The (effective) tier-k BS density, user density
R_k^z, $\mathcal{M}_k^z$	Distance between a tier-k BS and its selected user in link-z, tier-k heterogeneity parameter in link-z
$\hat{\lambda}_{k,l}$,$\hat{P}_{k,l}$, $\hat{A}_{k,l}$, $\hat{\kappa}_{k,l}^z$	Ratios of the density, transmit power, antenna gain, biasing factor in link-z between tiers k and l

II. System Model

Macro-cell BSs, whose location set is denoted as $\mathbf{Y}_m$, transmit with power P_m and receive signals with receiving antenna gain A_m and small-cell BSs, whose location set is denoted as $\mathbf{Y}_s$, transmit with power P_s and receive signals with receiving antenna gain A_s. In addition, mobile users, whose location set is denoted as $\mathbf{X}$, transmit with variable transmit power up to P_u and receive their signals with receiving antenna gain A_u. In the HCN, each user is associated with a BS per link (DL or UL). Let

Manuscript received July 26, 2014; revised September 16, 2014 and September 30, 2014; accepted October 1, 2014. Date of publication October 13, 2014; date of current version December 8, 2014. This research was supported by Basic Science Research Program through the National Research Foundation of Korea (NRF) funded by the Ministry of Education, Science and Technology (2013-024473) and in part by the ICT R&D program of MSIP/IITP (12-911-04-004). The associate editor coordinating the review of this paper and approving it for publication was C.-H. Lee.

The authors are with the Department of Electrical and Electronic Engineering, Yonsei University, Seoul 120-749, Korea (e-mail: ks.kim@yonsei.ac.kr).

Color versions of one or more of the figures in this paper are available online at http://ieeexplore.ieee.org.

Digital Object Identifier 10.1109/LCOMM.2014.2362757

$\mathbf{X}^D(\mathbf{y})$(or $\mathbf{X}^U(\mathbf{y})$), $\mathbf{y} \in \mathbf{Y} = \mathbf{Y}_m \cup \mathbf{Y}_s$, denote the set of users associated with BS $\mathbf{y}$ in DL (or UL). Then, $\mathbf{X}^z(\mathbf{y}) \bigcap \mathbf{X}^z(\mathbf{y}')$ is an empty set for $\mathbf{y} \neq \mathbf{y}'$ and $\bigcup_{\mathbf{y}\in\mathbf{Y}} \mathbf{X}^z(\mathbf{y}) = \mathbf{X}$ for $z \in \{D, U\}$. In the conventional cell association as in [2], $\mathbf{X}^D(\mathbf{y}) = \mathbf{X}^U(\mathbf{y})$ for all $\mathbf{y} \in \mathbf{Y}$. However, in this paper, it is assumed that each user can be associated with different BSs for DL and UL. Then, $\bigcup_{\mathbf{y}\in\mathbf{Y}_m} \mathbf{X}^z(\mathbf{y}) = \mathbf{X}_m$, $\bigcup_{\mathbf{y}\in\mathbf{Y}_s} \mathbf{X}^z(\mathbf{y}) = \mathbf{X}_s$ and $\mathbf{X}_s^z \bigcup \mathbf{X}_m^z = \mathbf{X}$.

To handle the cross-tier interference, the resource (time or frequency) is assumed to be partitioned as macro-cell dedicated resource, small-cell dedicated resource, and common resource, whose portions are respectively given as $0 \leq \zeta_m^z \leq 1$, $0 \leq \zeta_s^z \leq 1$, and $0 \leq \zeta_c^z = 1 - \zeta_m^z - \zeta_s^z \leq 1$. For each scheduling time, DL and UL data transmission using round-robin (RR) policy is assumed to be assigned to one of the available channels randomly. Also, the UL transmit power $P_u(\mathbf{x})$ of $\mathbf{x} \in \mathbf{X}$ is assumed to be selected among $\mathbf{P} = \{\mu_j P_u | 0 \leq \mu_1 \leq \ldots \leq \mu_J = 1\}$ to maintain the average received power at the associated BS $\mathbf{y} \in \mathbf{Y}_k$ above or equal to γ_k, i.e., the power control target in each tier can be different.

Let $\Gamma_{\mathbf{y},\mathbf{r}}^z$ denote the SIR between BS $\mathbf{y}$ and its selected user $\mathbf{x}^z(\mathbf{y})$ using resource $r \in \{c, d\}$, given by

$$\Gamma_{\mathbf{y},r}^z = \frac{P_{\mathbf{y}}^z h_{\mathbf{yy}} \Omega_{\mathbf{yy}} \left\|\mathbf{x}^z(\mathbf{y}) - \mathbf{y}\right\|^{-\alpha}}{\sum_{k\in\{m,s\}} 1(\mathbf{y} \in \mathbf{Y}_k) \left[I_m^z \;\; I_s^z\right] \mathbf{1}_{k,r}^T}, \tag{1}$$

where $P_{\mathbf{y}}^D = P_k A_u$, $P_{\mathbf{y}}^U = P_u(\mathbf{x}^U(\mathbf{y}))A_k$ for $\mathbf{y} \in \mathbf{Y}_k$, $I_l^D = \sum_{\mathbf{y}'\in\mathbf{Y}_l\setminus\mathbf{y}} P_l A_u h_{\mathbf{y}\mathbf{y}'} \Omega_{\mathbf{y}\mathbf{y}'} \|\mathbf{y}' - \mathbf{x}^D(\mathbf{y})\|^{-\alpha}$, $I_l^U = \sum_{\mathbf{y}'\in\mathbf{Y}_l\setminus\mathbf{y}} P_u(\mathbf{x}^U(\mathbf{y}'))A_k h_{\mathbf{y}'\mathbf{y}} \Omega_{\mathbf{y}'\mathbf{y}} \|\mathbf{x}^U(\mathbf{y}') - \mathbf{y}\|^{-\alpha}$, $1(\cdot) \in \{0, 1\}$ denotes the indicator function, and $\mathbf{1}_{k,c} = [1 \;\; 1]$ and $\mathbf{1}_{k,d} = [1 \;\; 0]([0 \;\; 1])$ if $k = m$ $(k = s)$. Here, $h_{\mathbf{yy}'}$ and $\Omega_{\mathbf{yy}'}$ denote the instantaneous channel gain and the shadowing gain between the user $\mathbf{x}^z(\mathbf{y})$ and BS $\mathbf{y}'$, which are modeled as a exponential random variable with unit mean and a log-normally distributed random variable, respectively, and α denotes the path loss exponent, $\alpha > 2$. Then, the DL $(z = D)$ or UL $(z = U)$ SIR distribution of tier $k \in \{m, s\}$ using resource $r \in \{c, d\}$ is defined as $\mathcal{S}_{k,r}^z(T) = \mathbf{E}[\mathbb{P}[\Gamma_{\mathbf{y},r}^z < T] | \mathbf{y} \in \mathbf{Y}_k]$, where $\mathbb{P}$ denotes the probability over channel realizations and $\mathbf{E}$ denotes the expectation over geometrical realizations.

III. Uplink SIR Distribution

A. Association Rule and Uplink Power Control

Let $P_{\mathbf{y}}$, $A_{\mathbf{y}}$ and $\kappa_{\mathbf{y}}^z$ denote the transmit power, antenna gain, and biasing factor of BS $\mathbf{y}$ and $\mathbf{y}^z(\mathbf{x})$ denote the associated BS of user $\mathbf{x}$ in link-z and $\Omega_{\mathbf{xy}}$ denote the shadowing gain between $\mathbf{x} \in \mathbf{X}$ and $\mathbf{y} \in \mathbf{Y}$. By adopting the best biased received signal power criterion for the association, the serving BSs for DL and UL can be respectively selected as

$$\mathbf{y}^D(\mathbf{x}) = \arg\max\nolimits_{\mathbf{y}\in\mathbf{Y}} P_{\mathbf{y}} \Omega_{\mathbf{xy}} A_u \kappa_{\mathbf{y}}^D \|\mathbf{x} - \mathbf{y}\|^{-\alpha}, \tag{2}$$

$$\mathbf{y}^U(\mathbf{x}) = \arg\max\nolimits_{\mathbf{y}\in\mathbf{Y}} P_u \Omega_{\mathbf{xy}} A_{\mathbf{y}} \kappa_{\mathbf{y}}^U \|\mathbf{x} - \mathbf{y}\|^{-\alpha}. \tag{3}$$

For analytical purposes, macro-cell BSs, small-cell BSs, and mobile users are assumed to be distributed according to PPPs with intensities $\bar{\lambda}_m$, $\bar{\lambda}_s$ and $\bar{\lambda}_u$, respectively. Also, similarly as in [7], the shadowing gain at each BS in a tier is assumed to be the same regardless of transmitters, i.e., $\Omega_{\mathbf{xy}}(\Omega_{\mathbf{y}'\mathbf{y}}) = \Omega_{\mathbf{y}}$, and to follow an independent and identical distribution according to its tier. Then, we can consider the shadowing effect as a random displacement on the BS locations in each tier [7] so that the effective BS location in tier-k becomes a PPP with $\lambda_k = \bar{\lambda}_k \mathbf{E}[\Omega_k^{2/\alpha}]$, $k \in \{m, s\}$. Note that dropping the shadowing gain in (1) does not change the SIR because all transmitters at each receiver have the same shadowing gain and the distribution of R_k^U, the distance between a BS and its randomly selected user, is given as $f_{R_k^U}(x) = 2\pi\lambda_k \mathcal{M}_k^U x \exp(-\pi\lambda_k \mathcal{M}_k^U x^2)$, where $\mathcal{M}_k^U = \hat{\lambda}_{\bar{k},k} (\hat{A}_{\bar{k},k} \hat{\kappa}_{\bar{k},k}^U)^{2/\alpha} + 1$, $\bar{k} \in \{m, s\} \setminus \{k\}$ for $k \in \{m, s\}$, $\hat{\lambda}_{k,l} = \lambda_k/\lambda_l$, $\hat{P}_{k,l} = P_k/P_l$, $\hat{A}_{k,l} = A_k/A_l$ and $\hat{\kappa}_{k,l}^z = \kappa_k^z/\kappa_l^z$, because the UL case is equivalent to the DL case [2], [7] with $\kappa_k^D = P_u A_k \kappa_k^U/(P_k A_u)$. Then, the distribution of the average gain between a BS and a randomly selected user is easily obtained as $f_{(R_k^U)^\alpha}(v) = (1/\alpha) v^{(1/\alpha - 1)} f_{R_k^U}(v^{1/\alpha})$ and the probability mass function (pmf) of the UL power control factor, $p_k^U(j) = \mathbb{P}[P_u(\mathbf{x}^U(\mathbf{y})) = \mu_j P_u]$, $j = 1, \ldots, J$, of a randomly selected $\mathbf{x}^U(\mathbf{y})$ of $\mathbf{y} \in \mathbf{Y}_k$ is given as

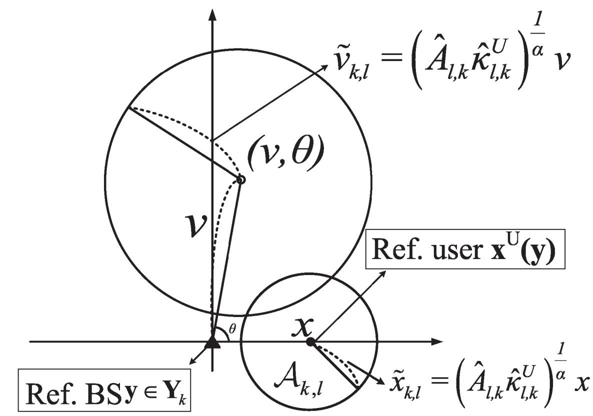

Fig. 1. The uplink interference region.

$$p_k^U(j) = \begin{cases} e^{-\lambda_k \mathcal{M}_k^U \left(\frac{\mu_{j-1} P_u}{\eta_k}\right)^{2/\alpha}} \\ \quad - e^{-\lambda_k \mathcal{M}_k^U \left(\frac{\mu_j P_u}{\eta_k}\right)^{2/\alpha}}, & j = 1, \ldots, J-1, \\ e^{-\lambda_k \mathcal{M}_k^U \left(\frac{\mu_{j-1} P_u}{\eta_k}\right)^{2/\alpha}}, & j = J, \end{cases} \tag{4}$$

where $\mu_0 = 0$ and $\eta_k = 10^{0.1\gamma_k} N_0/A_k$.

B. Uplink SIR Distribution

In Fig. 1, the region of possible interferers in UL is drawn using a polar coordinate where the reference BS $\mathbf{y} \in \mathbf{Y}_k$, $k \in \{m, s\}$, is located at the origin and its desired user $\mathbf{x}^U(\mathbf{y})$ is located at $(x, 0)$. Then, a tier-l BS cannot be located within the circle (denoted as $\mathcal{A}_{k,l}$) with radius of $\tilde{x}_{k,l} = (\hat{A}_{l,k} \hat{\kappa}_{l,k}^U)^{1/\alpha} x$ and centered at $(x, 0)$ because otherwise, the desired user does not belong to $\mathbf{y}$ any more. For the reference BS $\mathbf{y}$, the true UL interferer distribution and power distribution become highly non-uniform and even depend on the BS realizations. Because the exact distributions are too complex to be analyzed, it is assumed for mathematical tractability that the tier-l interferers to the tier-k reference BS locate at the origin are distributed according to an independent non-homogeneous PPP and each interferer power is independent and follows the pmf given in (4). Note that the intensity function of tier-l interferers to a tier-k BS at (v, θ) is given as the tier-l BS density λ_l (one interferer for each BS at a time) times the probability that at least one tier-l BS exists within the circle radius of $\tilde{v}_{k,l} = (\hat{A}_{l,k}\hat{\kappa}^U_{l,k})^{1/\alpha}v$ and centered at (v,θ) except the overlapped area with $\mathcal{A}_{k,l}$.[1] Such an independent non-uniform PPP assumption takes thenon-uniformity fully into account but ignores the dependence for mathematical tractability because the dependence is not quite strong. By considering the overlapped area, the intensity function of tier-l interferer to a tier-k BS at (v,θ), $\lambda_{k,l}(v)$, can be well approximated by using a curve-fitting as $\lambda_{k,l}(v) \simeq \lambda_l \min(\delta_{k,l}v, 1)$, where $\delta_{k,l} = (\pi\lambda_l/4)^{1/2}(1+(\hat{A}_{l,k}\hat{\kappa}^U_{l,k})^{1/\alpha})^{-0.1}(\hat{A}_{l,k}\hat{\kappa}^U_{l,k})^{-1/\alpha}$. Then, $\mathcal{S}^U_{k,r}(T)$ can be rewritten as

$$\mathcal{S}^U_{k,r}(T) \simeq 1 - \prod_{l\in B_{k,r}} \mathcal{L}_{I^U_l}\left(\frac{T}{\eta_k A_k}\right)\left(1 - e^{-\lambda_k \mathcal{M}^U_k \bar{x}^2_k}\right)$$
$$- 2\pi\lambda_k\mathcal{M}^U_k \int_{\bar{x}_k}^{\infty} \prod_{l\in B_{k,r}} \mathcal{L}_{I^U_l}\left(\frac{T(x/\bar{x}_k)^\alpha}{\eta_k A_k}\right) x e^{-\pi\lambda_k\mathcal{M}^U_k x^2}dx, \tag{5}$$

where $\bar{x}_k = (P_u/\eta_k)^{1/\alpha}$ is the maximum distance that the UL power control can compensate the pathloss in tier-k, $\mathcal{L}_{I^U_l}(s) = \mathbf{E}[e^{-sI^U_l}]$ denotes the Laplace transform of I^U_l, $B_{k,c} = \{m, s\}$ and $B_{k,d} = \{k\}$, and is well-approximated as follows.

Theorem 1: The SIR distribution $\mathcal{S}^U_{k,r}(T)$, for $k \in \{m, s\}$ and $r \in \{c, d\}$, between a randomly selected user $\mathbf{x} \in \mathbf{X}^U_{k,r}$ and its associated BS is well approximated as

$$\mathcal{S}^U_{k,r}(T) \simeq 1 - \mathcal{J}\left(T; \lambda_k\mathcal{M}^U_k, \bar{x}_k, \mathbf{\Delta}_k, \mathbf{P}, \mathbf{\Lambda}_{k,r}\right), \tag{6}$$

where

$$\mathcal{J}(T; s, x, \mathbf{\Delta}, \mathbf{P}, \mathbf{\Lambda}) = \left(1 - e^{-sx^2}\right)e^{-\mathbf{\Lambda}\mathbf{H}^T(T;x,\mathbf{\Delta},\mathbf{P})}$$
$$+ \underline{\chi}\Sigma^n_{i=1} w_i 2\pi s(\underline{\chi}y_i + \bar{\chi})e^{-\pi s(\underline{\chi}y_i+\bar{\chi})^2}e^{-\mathbf{\Lambda}\mathbf{H}^T(T;\underline{\chi}y_i+\bar{\chi},\mathbf{\Delta},\mathbf{P})},$$

$\underline{\chi} = \frac{\chi - x}{2}$, $\bar{\chi} = \frac{\chi + x}{2}$, $\mathbf{\Lambda}_{k,r} = [\lambda_m\ \lambda_s]diag(\mathbf{1}_{k,r})$, $\mathbf{\Delta}_k = [\delta_{k,m}\ \delta_{k,s}]$, $\mathbf{P} = [p^U_m\ \ p^U_s]$, and $diag(\mathbf{a})$ denotes the diagonal matrix with diagonal vector $\mathbf{a}$, and $\mathbf{H}(T; x, \mathbf{\Delta}, \mathbf{P})$ is as defined in Appendix A. Here, y_i and w_i respectively denote the ith root of the nth order Gauss-Legendre polynomials $P_n(y)$ [8] and the associated weight given as $w_i^{-1} = 0.5(1 - y_i^2)[P'_n(y_i)]^2$ and are respectively used as the sample points and their weights according to the n-point Gaussian quadrature rule [9] for sufficiently large χ.

Proof: See Appendix A. ■

IV. Simulation Result

For the simulation, the macro-cell BSs and users are generated according to PPPs with densities $\bar{\lambda}_m = 1$ BS/$(\pi(1.5\text{ km})^2)$ and $\bar{\lambda}_u = 300\bar{\lambda}_m$, respectively, over a circle with radius 50 km for each iteration and the results are collected over a circle with radius 10 km. The pathloss exponent is set to $\alpha = 4$ and $\Omega_m(\Omega_s)$ is assumed to be lognormally distributed with standard deviation of 8(10) [dB]. Also, an OFDMA (i.e., no intra-cell interference) is considered in which the channelization of each cell is identical and each subchannel independently selects a user for each scheduling time.

[1] When the interference from each interfering cell is averaged over G subchannels such as in a CDMA system, we can use $G\lambda_l$ instead of λ_l and scale each interfering power by a factor of $1/G$.

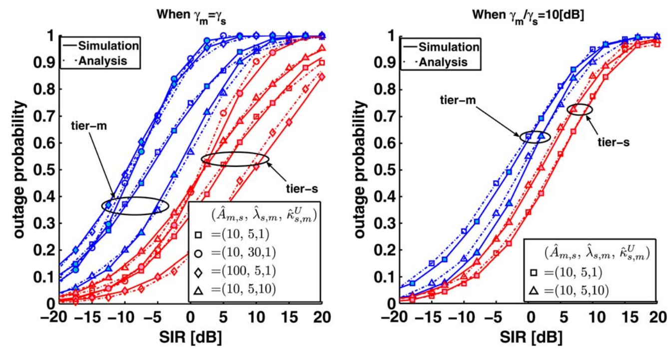

Fig. 2. The SIR distributions $\mathcal{S}^U_{m,c}(T)$ and $\mathcal{S}^U_{s,c}(T)$ in an HCN.

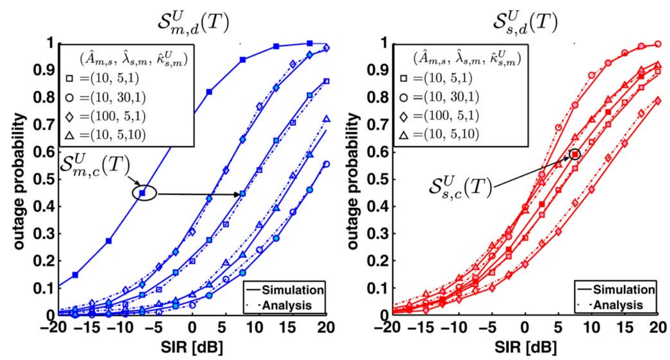

Fig. 3. The SIR distributions $\mathcal{S}^U_{m,d}(T)$ and $\mathcal{S}^U_{s,d}(T)$ in an HCN.

In Fig. 2, the UL SIR distributions using the common resource obtained from the simulations and those obtained from Theorem 1 are plotted for various values of the antenna gain ratio, $\hat{A}_{m,s}$, and the BS density ratio, $\hat{\lambda}_{s,m}$. Note that $\mathbf{E}[\Omega_m^{2/\alpha}]/\mathbf{E}[\Omega_s^{2/\alpha}] = 0.64$ so that $\hat{\lambda}_{s,m} = 0.64\bar{\lambda}_m/\bar{\lambda}_s$. Since each solid and dashed lines are quite close to each other in all cases, it is confirmed that the proposed UL SIR distributions are well matched to the true distributions and well reflect the trend of the true UL SIR distributions for various network parameters over almost entire range of practical interest ($\hat{A}_{m,s}$ up to 100 and $\hat{\lambda}_{s,m}$ up to few tens). Also, differently from the DL case, the SIR distribution in tier-m is much worse than that in tier-s because tier-m users suffer from strong interference from tier-s, which becomes worse as the BS density ratio increases (more strong interference), or the antenna gain ratio increases (increased statistical distance between a tier-m BS and its user). When a range expansion is applied to tier-s BSs, the statistical distance between a tier-m BS and its users decreases so that the tier-m SIR distribution is improved (i.e., shifts to the right so that the probability of SIR below a threshold is reduced) at the expense of the degradation (i.e., shifts to the left so that the probability increases) in the tier-s SIR distribution. Also, when different power control strategy is applied for each tier ($\gamma_m \geq \gamma_s$), the tier-m SIR distribution is improved due to the reduced interference power at the expense of the tier-s SIR distribution due to the reduced signal power.

In Fig. 3, the tier-m and tier-s UL SIR distributions using the dedicated resource (no cross-tier interference) are respectively plotted for various values of the antenna gain ratio and the BS density ratio as in Fig. 2. By comparing solid and dashed lines, it is again confirmed that the proposed UL SIR distributions are well matched to the true distributions and well reflect the trend of the true UL SIR distributions for various network parameters. Compared with those in Fig. 2, it is shown that the tier-m UL

SIR distributions are greatly improved by using a dedicated resource while tier-s UL SIR distributions are improved a little even when a cell range expansion is used. Thus, it would be much more beneficial to use dedicated resource for tier-m than does for tier-s in UL HCN.

As can be seen from Figs. 2 and 3, different power control strategy as well as resource partitioning (differently to the DL case [4], dedicated resource for tier-m), can be used for a load balancing in UL HCN. As a simple example, a load balancing is performed by utilizing the proposed framework, in which the average user throughput in each tier is maximized while satisfying i) similar outage probabilities for both tiers at target SIR T_0 and ii) the average throughput ratio within L between the two tiers. Here, the load balancing parameters are determined from the proposed framework and the outage probabilities and the average user throughputs are obtained from the simulations when the obtained load balancing parameters are applied. Let $\mathcal{O}_k^z$ and $\mathcal{T}_k^z$ denote the outage probability and the average throughput per user in link-z of tier-k, respectively. For a typical HCN with $\hat{P}_{m,s}=100$, $\hat{A}_{m,s}=10$ and $\hat{\lambda}_{s,m}=5$ between tiers, the UL outage probabilities are $(\mathcal{O}_m^U, \mathcal{O}_s^U)=(0.65, 0.12)$ while $\mathcal{O}_m^D=\mathcal{O}_s^D=0.2$ and the average throughputs per user are $(\mathcal{T}_m^D, \mathcal{T}_s^D, \mathcal{T}_m^U, \mathcal{T}_s^U)=(0.015, 0.140, 0.035, 0.100)$ [bps/Hz] without any load balancing, $T_o=-5$ [dB] and $\gamma_m=\gamma_s$. By setting the DL outage probability of 0.2 as a reference and $L=2$, the anticipated optimal load balancing parameters for UL are $(\hat{\kappa}_{s,m}^U, \gamma_m/\gamma_s, \zeta_m^U, \zeta_c^U)=(2.10, 8.91[\text{dB}], 0.11, 0.89)$ and the simulated result when the obtained load balancing parameters are applied gives $(\mathcal{O}_m^U, \mathcal{O}_s^U, \mathcal{T}_m^U, \mathcal{T}_s^U)=(0.20, 0.19, 0.043, 0.086)$, which confirms that load balancing parameter obtained by utilizing the proposed framework works well. In addition, the DL load balancing [4] for the same target gives $(\mathcal{O}_m^D, \mathcal{O}_s^D, \mathcal{T}_m^D, \mathcal{T}_s^D)=(0.19, 0.20, 0.049, 0.098)$, from which we can see that the UL load balancing performance can be comparable to that of the DL. Although not shown explicitly due to the space limitation, the proposed approach is still valid even when the pathloss exponent in each tier is different so that $\mathcal{S}_{k,r}^U(T)$ can be evaluated by using the Gaussian quadrature rule similarly as in Theorem 1 on the modified version of (5), which requires a simple numerical integration as in [2]. When $\alpha_m = 4$ and $\alpha_s = 4.5$ for tier-m and tier-s, respectively, the optimal UL load balancing parameters are change to $(\hat{\kappa}_{s,m}^U, \gamma_m/\gamma_s, \zeta_m^U, \zeta_c^U) = (2.80, 9.24[\text{dB}], 0.19, 0.81)$, which provides $(\mathcal{O}_m^U, \mathcal{O}_s^U, \mathcal{T}_m^U, \mathcal{T}_s^U) = (0.20, 0.19, 0.039, 0.078)$, which confirms that the proposed framework still works well even when the pathloss exponent in each tier is different.

V. Conclusion

In this paper, the UL SIR distributions are analyzed in a two-tier HCN and approximated closed-form SIR distributions are provided according to the tier, association rule, power control strategy in each tier and resource partition. The proposed SIR distributions are shown to be well-matched to the true distributions in a wide range of network parameters by comparing with the simulation results. Thus, the impact of applying different power control strategy or using dedicated resource for each tier on a UL HCN can be well described in terms of the proposed SIR distributions, which can be further utilized for the design of an HCN or devising association, resource allocation and load balancing schemes in an HCN. Future work includes the application of more practical scheduling or multiple antenna schemes on the proposed framework.

Appendix A

The two Laplace transforms in (5) can be written as $\mathcal{L}_{I_l^U}(\frac{T(x/\bar{x}_k)^\nu}{\eta_k A_k})$ for $\nu=\{0,\alpha\}$, and can be approximated as

$$\mathcal{L}_{I_l^U}\left(\frac{T\bar{x}_k^\nu}{\eta_k A_k}\right)$$
$$\simeq \exp\left(-\int_0^{2\pi}\int_0^\infty \lambda_{k,l}(v)\left(1-\mathbf{E}_{\mu,h}\left[\exp\left(-\frac{T(x/\bar{x}_k)^\nu \mu P_u h}{\eta_k v^\alpha}\right)\right]\right) v dv d\theta\right)$$
$$= \exp\left(-2\pi\lambda_l\left(\int_0^{\delta_{k,l}^{-1}} \delta_{k,l}\mathbf{E}_\mu\left[\left(1+\left(\frac{\eta_k v^\alpha}{T(x/\bar{x}_k)^\nu \mu P_u}\right)\right)^{-1}\right] v^2 dv \right.\right.$$
$$\left.\left. + \int_{\delta_{k,l}^{-1}}^\infty \mathbf{E}_\mu\left[\left(1+\left(\frac{\eta_k v^\alpha}{T(x/\bar{x}_k)^\nu \mu P_u}\right)\right)^{-1}\right] v dv\right)\right), \tag{7}$$

where μ denotes a random variable denoting the UL power control factor of an interferer having pmf as given in (4) and h denotes an exponential random variable with unit mean denoting the fading channel. Using (4), (7) can be obtained as

$$\mathcal{L}_{I_l^U}\left(\frac{T(x/\bar{x}_k)^\nu}{\eta_k A_k}\right)$$
$$\simeq \exp\left(-2\pi\lambda_l \Sigma_{j=1}^J \left(\int_0^{\delta_{k,l}^{-1}} \frac{\delta_{k,l} v^2}{1+q_{k,j} v^\alpha} dv \right.\right.$$
$$\left.\left. + \int_{\delta_{k,l}^{-1}}^\infty \frac{v}{1+q_{k,j}v^\alpha} dv\right) p_k^U(j)\right)$$
$$= \exp\left(-\left([\lambda_m\ \lambda_s]\right)_l \left(\mathbf{H}(T;x,\mathbf{\Delta},\mathbf{P})\right)_l\right), \tag{8}$$

where $q_{k,j}=\eta_k/(T(x/\bar{x}_k)^\nu \mu_j P_u)$, $\mathbf{H}(T;x,\mathbf{\Delta},\mathbf{P})=[\mathcal{H}(T;x,(\mathbf{\Delta})_1,(\mathbf{P})_1)\mathcal{H}(T;x,(\mathbf{\Delta})_2,(\mathbf{P})_2)]$, and $\mathcal{H}(T;x,\delta,p) = 2\pi\Sigma_{j=1}^J((\delta^{-2}/3)\,{}_2F_1[1,3/\alpha;1+3/\alpha;-(T\mu_j(x\delta)^\alpha)^{-1}] + T\mu_j x^\alpha \delta^{\alpha-2}/(\alpha-2)\,{}_2F_1[1,1-2/\alpha;2-2/\alpha;T\mu_j(x\delta)^\alpha])p(j)$, where $(\mathbf{a})_l$ denotes the lth element of a vector $\mathbf{a}$, and ${}_2F_1[.]$ denotes the hypergeometric function [9]. Here, the second equality comes from the facts that $\int_0^a \frac{v^2}{1+bv^\alpha}dv = \frac{a^3}{3}\,{}_2F_1[1,\frac{3}{\alpha};1+\frac{3}{\alpha};-ba^\alpha]$ and $\int_a^\infty \frac{v}{1+bv^\alpha}dv = \frac{b^{-1}a^{2-\alpha}}{\alpha-2}\,{}_2F_1[1,1-\frac{2}{\alpha};2-\frac{2}{\alpha};-b^{-1}a^{-\alpha}]$. By inserting (8) into (5), the integrand becomes the form of $xe^{g(x)}$ with a polynomial function $g(x)$ so that it can be approximated by using the n-point Gaussian quadrature rule [9] with Gauss-Legendre polynomials [8] as in Theorem 1.

References

[1] S. Parkvall, A. Furuskar, and E. Dahlman, "Evolution of LTE toward IMT-advanced," *IEEE Commun. Mag.*, vol. 49, no. 2, pp. 84–91, Feb. 2011.

[2] H. Jo, Y. J. Sang, P. Xia, and J. G. Andrews, "Heterogeneous cellular networks with flexible cell association: A comprehensive downlink SINR analysis," *IEEE Trans. Wireless Commun.*, vol. 11, no. 10, pp. 3484–3495, Oct. 2012.

[3] Y. J. Sang and K. S. Kim, "Load distribution in heterogeneous cellular networks," *IEEE Commun. Lett.*, vol. 18, no. 2, pp. 237–240, Feb. 2014.

[4] S. Singh and J. G. Andrews, "Joint resource partitioning and offloading in heterogeneous cellular networks," *IEEE Trans. Wireless Commun.*, vol. 13, no. 2, pp. 888–901, Feb. 2014.

[5] T. D. Novlan, H. S. Dhillon, and J. G. Andrews, "Analytical modeling of uplink cellular networks," *IEEE Trans. Wireless Commun.*, vol. 12, no. 6, pp. 2669–2679, Jun. 2013.

[6] V. Chandrasekhar and J. G. Andrews, "Uplink capacity and interference avoidance for two-tier femtocell networks," *IEEE Trans. Wireless Commun.*, vol. 8, no. 7, pp. 3489–3509, Jul. 2009.

[7] H. S. Dhillon and J. G. Andrews, "Downlink rate distribution in heterogeneous cellular networks under generalized cell association," *IEEE Trans. Wireless Commun.*, vol. 3, no. 1, pp. 42–45, Nov. 2013.

[8] W. H. Press, S. A. Teukolsky, W. T. Vetterling, and B. P. Flannery, *Numerical Recipes: The Art of Scientific Computing*, 3rd ed. Cambridge, U.K.: Cambridge Univ. Press, 2007.

[9] A. Gil, J. Segura, and N. M. Temme, *Numerical Methods for Special Functions*, 1st ed. Philadelphia, PA, USA: SIAM, 2007.